Journal of Fundamental and Applied Sciences

Research Article

ISSN 1112-9867

Available online at http://www.jfas.info

MONTE CARLO SIMULATION OF INTERACTION BETWEEN AN ELECTRON BEAM AND A NANO-SILICON FILM

Z. Elateche[1] and M.S.Aida[2]

[1]Department of physics, Faculty of science, Batna 1 University, Batna, Algeria

[2]Department of physics, King abdulaziz University, Jeddah, Kingdom of saudi Arabia

Received: 11 September 2018 /Accepted: 17 December 2018 / Published online: 01 January 2019

ABSTRACT

Due to the fundamental role played by the interaction electron-matter in scanning electron microscopy (Electron Beam Induced Current -EBIC- in silicon case), a Monte Carlo calculation model of this interaction applied in silicon nanostructure is presented in the present paper. After a brief introduction to scattering process, our model procedure is described in which electron trajectories in the sample, penetration range (in depth and in spread), backscattered and secondary electron yields (the total electron yield) for nanostructure of silicon are calculated. The variation of this parameters with angle of incidence and impact energy have been studied.

The validation of our model is performed by means of comparison with results which been reported by various authors.

Keywords: Monte Carlo method; EBIC; silicon; nano-structure; Electron emission yield.

Author Correspondence, e-mail: z.elateche@yahoo.fr

http://dx.doi.org/10.4314/jfas.v11i1.19

1. INTRODUCTION

The interaction of electron beams with solids has been studied for a long time because of interest in both the fundamentals of the interaction mechanisms and predicting the total electrons emission yield (EEY) [1-6]. In this work, this interaction is described by a Monte Carlo model.

Due to the rapid growth of technology a great variety of materials is used nowadays in the nanotechnology industry. We will confine ourselves, however, to one important material in particular, i.e. Silicon, with his interesting properties. Monte Carlo simulations can be used to predict these parameters.

First, the principle fundamental considerations about the scattering process is briefly described. Next, the model is described also, the simulation results (trajectories, the electrons penetrations, EEY) in silicon's nanostructure are presented finally. The numerical results of the calculations are compared with others reported in the literature.

2. FUNDAMENTALS

2.1. Electrons trajectory

The electron-matter interaction during EBIC analysis may results in a range of effects on incident electrons, which can be divided into two primary types of electron scattering: elastic and inelastic. At low energy, one has to take into account not only the inelastic scattering (i.e., collision with electrons), but also the elastic scattering (i.e., deflection by nuclei) predominant in this energy ranges. In elastic scattering, the incident electrons is deflected to a new trajectory with now energy loss.

Our model is based on the widely accepted Monte Carlo model by Browning and al. [7]. In this model, the scattering angles θ (polar angle) and φ (azimuth angle) are defined by [8],

$$\cos\theta = 1-(2\beta R_1-(1+\beta- R_2)) \quad (1)$$ (Rutherford scattering)

In this equation that can generate a unique scattering angle θ in the rage of $[0,\pi]$.

$$\varphi = 2\pi R_3 \quad (2)$$

φ can be in the range $[0,2\pi]$. R_1, R_2 and $R3$ are a random number in the range [0,1] drawn automatically by computer after injection a germ n.

The atomic screening parameter derived by Wenzel, β, is defined as [9],

$$\beta = 3.4\ 10^{-3}\ Z^{0.67}\ E^{-1} \quad (3)$$

Where Z is the atomic number and E is the energy of the electron (in KeV).

The total average mean free path between scattering events, is defined by,

$$(1/\lambda_{Tot}) = (1/\lambda_e) + (1/\lambda_i) \quad (4)$$

The path length S between any scattering events has the Poisson distribution [10],

$$P(s) = \lambda_{Tot}^{-1}\ \ e^{-s/\lambda Tot} \quad (5)$$

and can be obtained with a uniform random number $R_4 \in [0,1]$ via the relation [11],

$$S = -\lambda_{Tot}\ ln\ (R_4) \quad (6)$$

Where λ_e is the mean free path for elastic scattering given by [12],

$$\lambda_e = A / (N_a\ \rho\ \sigma_{elas}) \quad (7)$$

A is the atomic weight of the target material [g/mol], ρ is the density [g/cm^3], and N_a is the Avogadro's number. The total elastic cross section σ_{elas} [cm^2 /atom] is obtained by [8],

$$\sigma_{elas} = [5.21\ 10^{-21}\ (Z/E)^2\ ((E+511)] / [(E+1024))^2\ (4\pi\ \beta / \beta\ (\beta+1))] \quad (8)$$

In the other hand and for inelastic scattering the mean free path for silicon is given by [13],

$$\lambda_i = E / [257.23\ (0.03\ ln\ (0.125\ E) - (1.66/E) + (46.49\ E^2)] \quad (9)$$

Where E [eV] and λ_i [°A].

2.2. Maximum penetration range

In a solid, each electron has an individual trajectory. The path electron length of this trajectory is the total distance traveled until the electron comes to rest. The average path length is known as the "range" of the electrons in the solid. The total length of an individual electron "random walk" trajectory is known as Bethe range [14],

$$R_e = \int_{E_0}^{0} dE \quad (10)$$

The effective depth to which energy dissipation extends is much smaller and its known as penetration range, it is given by this general formula [14]:

$$R_e = (K/\rho)\ (E_0)^{\gamma} \quad (11)$$

Where K depends on the atomic number and is also a function of energy, γ depends on the atomic number and on E_0.

2.3. Electron emission yoeld

The EEY is defined as the ratio between the number of electrons emitted by a solid over the number of electrons initially impacting this solid.

2.3.1. Backscattered electrons

The backscattered electrons are primary electrons that have undergone inelastic energy losses. The electrons that have been backscattered after experiencing a single inelastic interaction will get out of the target material.

2.3.2. Secondary electrons

The number of secondary electrons produced at a distance z from the surface $n(z,E)$ can be assumed to be proportional to the average rate of energy loss, so[15]:

$$n(Z,E) = (-1/\varepsilon)\,(dE/dz) \qquad (12)$$

Where ε, is the energy required to produce a secondary electron. The SE yield can be obtained as follows [16]: $\delta(E_0) = Const\,(E_0/\varepsilon)\,(\mu/R_e)\,(1-e^{-Re/\mu})$ (13)

μ is the mean electron escape depth.

3. Model

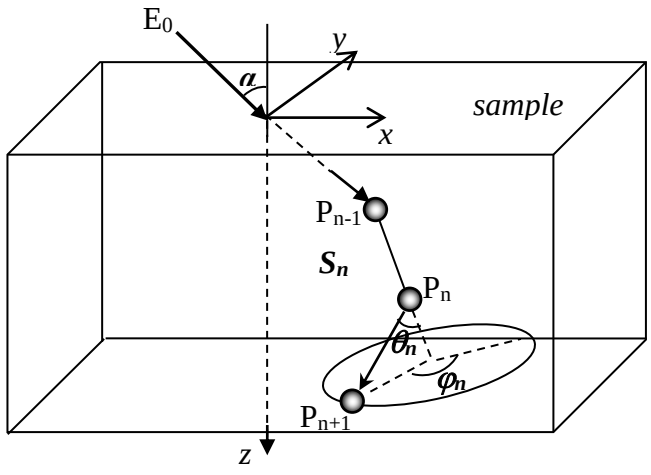

Fig.1. Schematic drawing to illustrate the present model for Monte Carlo simulation of electron penetration in sample

Let us consider an electron beam with n_{ele} incidents electrons and energy E_0 incident on a homogenous unsupported silicon nano-film in the $+z$ direction.

From (Figure 1) we obtained:

$$\cos\theta_{n+1} = \cos\theta_n \cos\theta - \sin\theta_n \sin\theta \cos\varphi \qquad (14)$$

$\sin(\varphi_{n+1} - \varphi_n) = (\sin\theta \sin\varphi) / \sin\theta_{n+1}$ (15)

$\cos(\varphi_{n+1} - \varphi_n) = (\cos\theta - \cos\theta_{n+1} \cos\theta_n) / \sin\theta_{n+1} \sin\theta_n$ (16)

(θ_{n-1}) and (φ_{n-1}) denote the direction of motion of an electron before scattering and (θ_n) , (φ_n) are its direction just after scattering through the scattering angle θ and φ being the azimuthal scattering angle (eq.1 and 2).

The electron goes forward one step with a defined orientation and its position at the next scattering point is defined by:

$x_{n+1} = x_n + S_n (\sin \theta_n \cos\varphi_n)$ (17)

$y_{n+1} = y_n + S_n (\sin \theta_n \sin\varphi_n)$ (18)

$z_{n+1} = z_n \cos\theta_n$ (19)

The type of scattering for each scattering event is selected by using a random number R_5 according to the relation: if $R5 \leq (1/\lambda_e) / (1/\lambda_i)$ the scattering is elastic, and vice versa.

We suppose to the first scattering was elastic.

Paths, energy losses and secondary electrons are calculated until the electron is emitted out of the solid or until its energy falls under an energy threshold. This threshold equals $e\chi+E_g+\Delta V$ for semiconductors, with E_g the energy bandgap, $e\chi$ the electron affinity and ΔV the valence [14], for Silicon this value is 50eV.

3.1. Maximum penetration range

3.1.1 In the depth

The electron range is measured of the straight-line penetration of electrons in a target.

We have determined the range R_e by:

$$R_e = \frac{\sum_{i=1}^{nele} (r_{\max})_i}{n_{ele}} \quad (20)$$

Where $(r_{max})_i$: the maximum distance traversed by the *i* electron.

3.1.2. In spread

In penetration in spread, we have calculated this Value Y_{max} (E_0) by the relation:

$$Y_{\max} = \frac{\sum_{i=1}^{nele} y_i}{n_{ele}} \quad (21)$$

where y_i is the position of the electron on (Y) axis.

3.2. Secondary yield

In order to be able to apply our model, the values of the parameters ε and μ must be known. We used Joy [17] values: For Silicon ε = 70 eV and μ =3.0 nm.

The range is then divided into fifty zones of equal length. in each collision the energy loss is $\Delta E = E_{e\text{-}h}$, where $E_{e\text{-}h}$ is the average energy of an electron-hole pair production. And in each zone, a quantity of pairs is generated.

The program was executed by changing target material and beam parameters.

4. RESULTS AND DISCUSSION

In all graphs, the angle of incidence (tilt) α (in degrees, 0≤ α < 90) is the angle between the vector of the incident beam and the normal vector to the sample surface.

4.1. Electrons trajectories

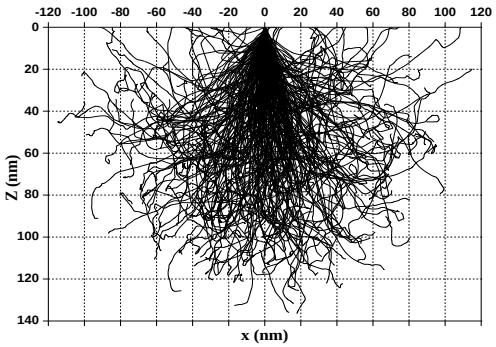

Fig.2. Trajectories of 250 electrons for 3 KeV

An example of simulation calculation is shown in Figure.2, where plots of 250 trajectories with E_0= 3 KeV.

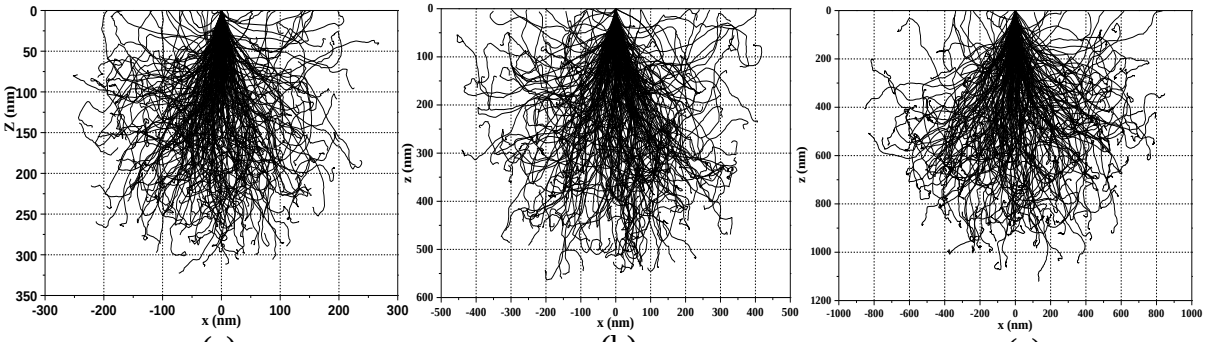

(a) (b) (c)

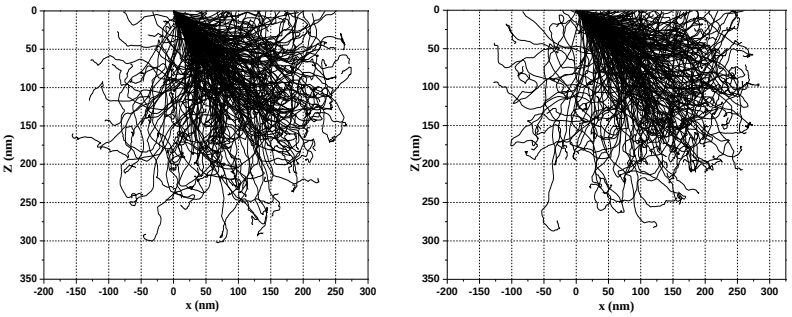

Fig.3. Trajectories of 200 electrons for (a) 5 KeV, (b) 7 KeV, (c) 10 KeV with tilt angle=0°, and (d) tilt =45°, (e) tilt =60° for E_0=5 KeV

Figure.3 (a), (b) and (c) depicts an illustration of the trajectories of 200 electrons as a function of primary energy (E_0 =5, 7, and 10 KeV) through Silicon nano-film. It is noticed that the generation volume takes the pear shape, which is the form considered by all the researchers in the case of Silicon. As the primary energy beam increases, the incident electrons penetrate into the sample along a path close to their incident direction, as they lose energy by inelastic scatterings the probability of elastic scatterings increase so they begin deflected into the sample.

Figure.3 (a), (d), and (e) illustrate the effect of the tilt (α=0°,45°, and 60°) angle on electrons trajectories (interaction volume). This angle is between the sample surface and the horizontal plane, determines the symmetry of the interaction volume; as the sample is tilted away from the horizontal the interaction volume appears asymmetric.

4.2. Electron range

Figure.4 presents the maximum penetration (in depth (a) and in the spread (b)) of electrons calculated for different values of primary energy E_0. This maximum increase when E_0 increases because the distance traveled by the primary electron inside a specimen before it loses all of its kinetic energy increases with the increase of E_0. Our simulation results show excellent agreement with the vast majority results of authors [18-21].

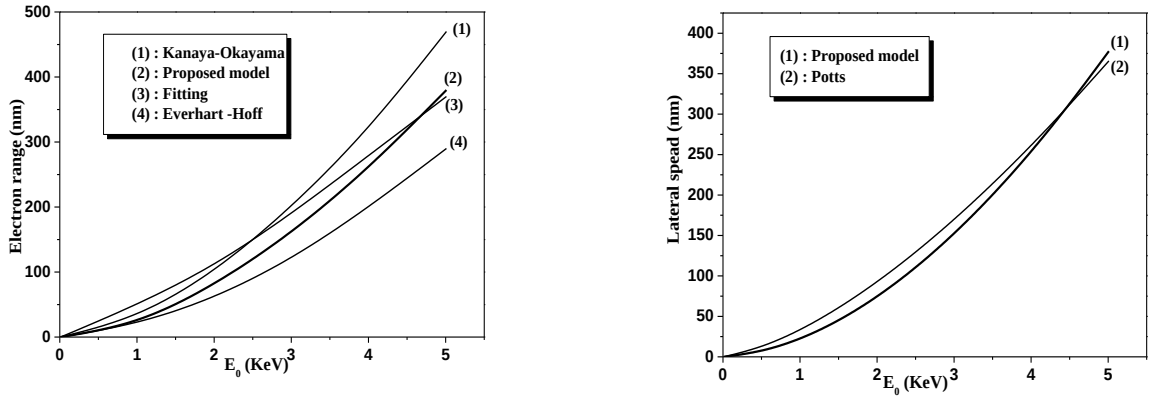

(a) (b)

Fig.4. The maximum penetration of electrons (a) in depth (z (E_0)) and (b) in spread (y (E_0))

4.3. Backscattered electrons

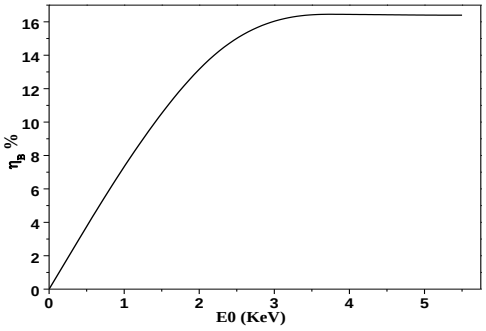

Fig.5. η_B versus E_0 for normal incidence ($\alpha = 0°$).

Figure.5, shows the variation of the electron backscatter coefficient η_B with the incident electron energy E_0 for normal incidence ($\alpha = 0°$). A slight increase of η_B with E_0 in low energies is showed, but in high energies there are a monotone form. The rational is that, for low energy there are an increase backscattered electron produced during the random walk. But after a E_0 value (2.2 KeV in our case) there is not a more backscattered electrons produced, but there is only a absorbed and transmitted electrons.

Figure.6 shows the average energy of the backscattered electrons as a function of E_0. In our model it's simply to calculate this value by the division of their energies amount by their total numbers. There is a good agreement between our results and this of Sternglass [22].

Figure 7 compares our Monte Carlo results with Arnal [23] and Drescher [24] data for the variation of η_B with α. The value of η_B monotonically increases with α. This is because as α increases, the portion of the forward-peaked differential elastic scattering distribution that falls in the backscatter volume increases, and thus more electrons can backscatter out of the sample, which leads to an increase in η_B.

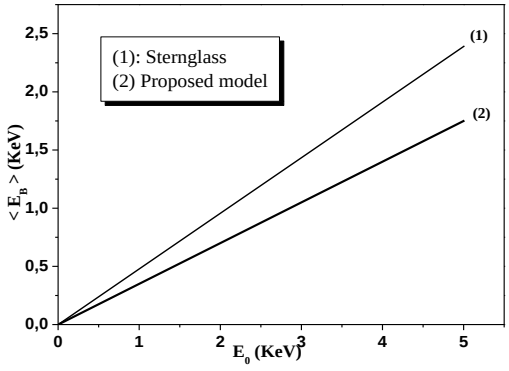

Fig.6. <E_B> versus E_0 for normal incidence ($\alpha = 0°$).

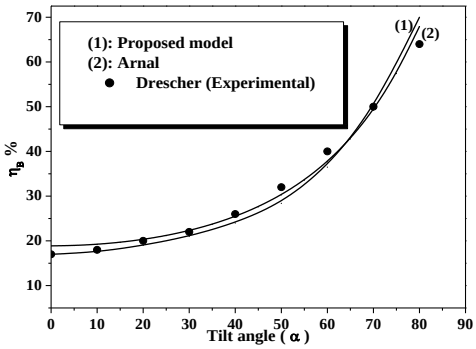

Fig.7. η_B versus α

4.4. Secondary electron emission

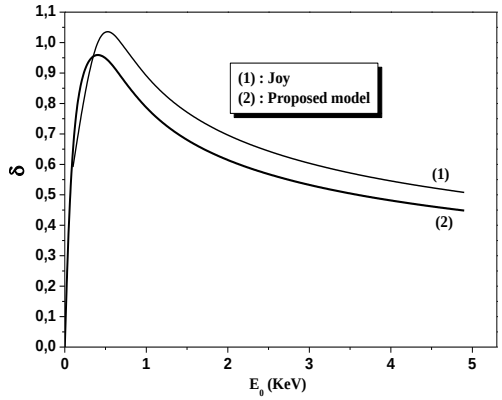

Fig.8. Secondary yield versus E_0

Figure 8 compares our results with Joy [17] data. Our calculation coincides very good with this data. Secondary electron yield is very important on low energies (the energies used in the nano-structures cases), but it is negligible for medium and high energies. Because the same reason of the backscattered electrons, after a certain value of E_0 there is only a absorbed and transmitted electrons.

4.5. The total Electrons Emission Yield (EEY)

The total yield is defined by [17]: $\sigma = \delta + \eta_B$ (22)

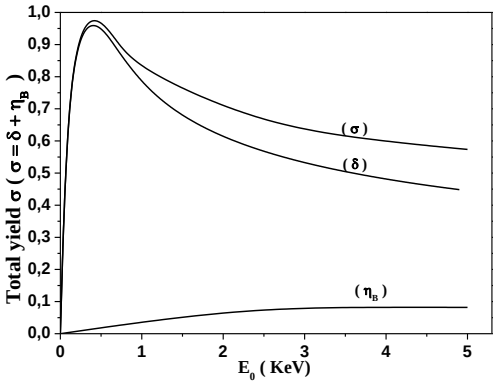

Fig.9. The total yield versus E_0

Figure.9, shows the variation of the total emission yield with the incident electron energy E_0 for normal incidence ($\alpha = 0°$). For a nano-film (low energies) Silicon σ depends greatly on δ (secondary yield).

5. CONCLUSION

A numerical model based on Monte Carlo method for interaction of an electron beam with a silicon nano-film is developed.

We have successfully applied this model to calculate the majority parameters of this interaction (trajectories, electron range, backscattering, secondary yield, and the total electrons emission yield).

For a Silicon nano-film, we found that, the trajectories, backscattered, and secondary electrons are influenced by the primary energies specially at low energies and by the tilt angle. In the other hand, the total yield depends greatly on (secondary yield).

We demonstrated that, this calculated is in good agreement with other results.

After this accepted result, this work proposes to extend the domain of validity of such kind of approaches to different materials and for kinetic energy [few eV-hundreds of keV].

6. REFERENCES

[1] K. G. McKay, *Recent Advances in electronics*, Academic, New York, p.56 (1948).

[2] E. M. Baroody, Phys. ReV. 78, p.780 (1950).

[3] A. J. Dekker, Phys. ReV. Lett.4, p.55 (1960).

[4] C. G. H. Walker, M.M. El-Gomati, A.M.D. Assa'ad, and M. Zadaražil, Scanning.30, p.365 (2008).

[5] L. Reimer, *Physics of image formation and microanalysis*, Springer.45, Berlin, p.135 (1998).

[6] D.C, Joy, Oxford University press.9, New York, p.25 (1995).

[7] R. Browning, T.Z. Li, B. Chui and Z. Czyzewski, *Scanning*. 17, p. 250 (1995).

[8] D.E. Newbury, D.C. Joy, P. Echlin and J.I. Goldstein, Advanced Scanning Electron Microscopy and X-Ray Microanalysis, Plenum Press, New York (1986)

[9] G. Wenzel, J.Appl.Phys.40, P.590 (1927).

[10] K. Tokesi, T. Mukoyama, Bull.Inst.Chem. Res. Kyoto University.72, p.4 (1994).

[11] I. Adesida, R. Shimizu and T.E. Everhart, J.Appl.Phys.51, p.596 (1980).

[12] E. Bauer, J. Vac. Sci. Technol.7, (1970).

[13] S. Tanuma, C.J. Powell and D.R. Penn, Surf.Interf.Anal.20, p.77 (1993).

[14] B.G. Yakobi, D.B. Holt, *Cathodoluminescence microscopy of inorganic solids*, Plenum Press, (1990).

[15] H. Salow, J.Appl.Phys.41, p.434 (1940).

[16] J. R. Young, Phys.Rev.103, pp.292.299 (1956).

[17] D.C. Joy, J. Microscopy.147, pp.51-64 (1987).

[18] K. Kanaya, S. Okayama, J.Phys. Appl.5, p.43(1972).

[19] H.J. Fitting, Phys.Stat.Sol. 26, p.25 (1974).

[20] T.E. Everhart, P.H. Hoff, J.Appl.Phys.42, p.37 (1971).

[21] A. Potts, J.Appl.Phys.5, pp.36-39 (1987).

[22] E.J. Sternglass, Phys. Rev. 95, p.345 (1954).

[23] F. Arnal, P.D. Vincinsini, C.R. Acad.Sci. Paris.1526, p.286 (1969).

[24] H. Drescher, L. Reimer, Angrew. Phys.German.29, p.331 (1970).

How to cite this article:
Z. Elateche, MS. Aida. Monte Carlo simulation of interaction between an electron beam and a nano Silicon film. J. Fundam. Appl. Sci., 2019, *11(1), 294-304.*